Analytical and Bioanalytical Chemistry
https://doi.org/10.1007/s00216-020-02886-0

RESEARCH PAPER

Fiber organic electrochemical transistors based on multi-walled carbon nanotube and polypyrrole composites for noninvasive lactate sensing

Yang Zhang[1] · Yuedan Wang[1] · Xing Qing[1] · Yao Wang[1] · Weibing Zhong[1] · Wenwen Wang[1] · Yuanli Chen[1] · Qiongzhen Liu[1] · Mufang Li[1] · Dong Wang[1]

Received: 11 May 2020 / Revised: 3 August 2020 / Accepted: 14 August 2020

Abstract

Multi-walled carbon nanotubes (MWCNT) play a synergistic role with conducting polymer in practical applications such as biological sensing. In this paper, multi-walled carbon nanotube and polypyrrole (PPy) composites were prepared on a fiber surface for the first time, and their morphology and electrical properties were characterized. Compared with PPy-coated fiber, the presence of carbon nanotubes induced the growth of large areas of PPy nanowires. In addition, fiber organic electrochemical transistors (FECTs) based on PPy and MWCNT were assembled, showing a higher on/off ratio, better stability, and greater flexibility. The lactate biosensor based on FECTs exhibits high sensitivity, with a correlation coefficient of $R = 0.9889$, quick response time of 0.6–0.8 s, a wide linear response range of 1 nM–1 mM, and excellent selectivity for lactate. Furthermore, the lactate concentration in human sweat was successfully detected by a FECT-based sensor. The hybrid fibers can be easily woven and placed on fabric simply by stitching. This favorable performance of the FECT-based sensor makes it suitable for noninvasive sensing of lactate. Therefore, it provides a promising platform for future use in healthcare and detection applications.

Keywords Multi-walled carbon nanotube · Electrochemical transistor · Flexibility · Lactate sensor · Fiber

Introduction

The determination of lactate is of great significance for clinical diagnostics, fermentation, and food analysis [1, 2]. In particular, lactate concentration is a key parameter in clinical diagnostics for predicting multiple organ failure and evaluating the health status of patients, such as monitoring respiratory insufficiency, metabolic disturbance, and psychological disorders [3–5]. Traditionally, chromatography and spectrophotometry have been used to analyze lactate concentrations [6–10]. However, these methods are time-consuming, expensive, and complicated. Therefore, the development of methods for the rapid, efficient, and real-time monitoring of lactate concentration is critical. Electrochemical biosensors can provide quantitative information. Specifically, organic electrochemical transistors (OECTs) show great potential in biomolecule detection due to their unique structure, small size, and compatibility with aqueous solution [11, 12]. In addition, most studies have indicated that OECT sensors are much more sensitive than traditional sensors, which is attributed to their inherent amplification characteristics and enhanced signal-to-noise ratio [13]. Khodagholy et al. [14] developed a planar organic electrochemical transistor consisting of two parallel strips of poly(3,4-ethylenedioxythiophene)/poly(styrenesulfonate) and ionic liquid for the detection of lactate concentration (10–100 mM). Ji et al. [15] reported an OECT-based glucose and lactate sensor in which the gate electrodes were modified with glucose oxidase/lactate oxidase and poly(n-vinyl-2-pyrrolidone)-capped platinum nanoparticles. The OECT sensors demonstrated extremely high sensitivity, with detection limits of glucose and lactate up to 100 nM and 1 uM, respectively. Strakosas et al. [16] developed enzymatic sensors using a

Electronic supplementary material The online version of this article (https://doi.org/10.1007/s00216-020-02886-0) contains supplementary material, which is available to authorized users.

✉ Yuedan Wang
wydan2015@163.com

✉ Dong Wang
wangdon08@126.com

[1] Hubei Key Laboratory of Advanced Textile Materials & Application, Wuhan Textile University, Wuhan 430200, Hubei, China

Published online: 30 August 2020

platinum-modified gate of a planar OECT. The sensors showed high stability, sensitivity, and selectivity, although the planar configuration and long response time were not conducive to practical application.

Fiber is bendable and elastic, which makes it easy to be woven and integrated into fabrics. Fiber can also be used to develop electronic components on textile substrates to achieve better function, transforming traditional two-dimensional structures for three-dimensional detection. In our previous study, FECTs were integrated to produce glucose and dopamine sensors [17, 18]. Owing to the flexibility and structural uniqueness, FECTs exhibit superior sensitivity and excellent selectivity, while maintaining good repeatability. Conducting polymers have been studied extensively in OECTs, and make it possible to prepare large-area flexible devices. Among these, polypyrrole (PPy) has captured considerable attention because of its redox properties, variable conductivity, and ease of preparation [19–21]. However, its widespread use is limited because of poor stability and short cycle life [22, 23]. At the same time, carbon nanotubes (CNT) have been widely studied given their high surface activity, chemical and electrochemical stability, acceptable biocompatibility, and rapid electron transfer kinetics [24, 25]. However, many studies have reported that CNTs lack selectivity and require metal oxides or conducting polymers to enhance their specificity. Therefore, considerable efforts have been carried out recently to prepare CNT and conducting polymer nanocomposites for biological sensing. Cui et al. [26] reported the biocatalytic synthesis of a PPy-enzyme-CNT composite, and the prepared nanocomposites were successfully applied for an electrochemical biosensor of lactate. Braik et al. [27] prepared a poly(3,4-ethylenedioxythiophene)/CNT-modified electrode and investigated a highly sensitive amperometric enzyme biosensor for superoxide detection. Because of the synergistic effects, the biosensor presented better analytical performance, higher sensitivity, and lower detection limit. Xue et al. [28] described a flexible polyaniline/CNT nanocomposite film-based electronic gas sensor. Compared with CNT- and polyaniline-based films, the hierarchical nanocomposite film sensor exhibited better sensing response and cycle stability. All these results indicate that the synergistic effects of composites significantly enhance the electrochemical properties.

In this study, multi-walled carbon nanotubes (MWCNT) were first coated on the backbone of nylon (PA6) fiber, forming a thin template and conductive layer. The pyrrole was then polymerized in situ on the surface of the MWCNT-modified PA6 fiber, forming a large number of PPy nanowires to enhance the electrical properties and electrochemical activity. The transistors were assembled from the composite materials as the channel layer, electrode, and solid electrolyte, which is more conducive to wearable electronic biosensor devices. The electrical properties and sensor performance of the devices were investigated. The FECT-based sensor demonstrated a better sensing response and was easily integrated into fabrics, providing great potential for point-of-care applications.

Experimental section

Materials

PA6 filament, acetone, alcohol, sodium dodecyl benzene sulfonate, pyrrole, 5-sulfosalicylic acid dihydrate, iron(III) nitrate nonahydrate, sodium anthraquinone-2-sulfonate, poly(vinyl alcohol) (PVA), glucose, ascorbic acid (AA), creatinine, uric acid (UA), phosphate, and multi-walled carbon nanotubes were purchased from Aladdin Reagent Co. L-(+)-lactic acid and LO_X (from *Pediococcus* sp. lyophilized powder, ≥20 units/mg solid) were obtained from Sigma-Aldrich (USA). Nafion (D520) was supplied by Shanghai Hesen Electric Co., Ltd. LO_X stock solution (10 mg/mL) was prepared with phosphate-buffered saline (PBS, pH = 6.5). All the reagents in this study were of analytical grade and were used as received.

Preparation of PPy nanowire/MWCNT/PA6 fiber and PPy/PA6 fiber

First, the 85D (D represents denier) PA6 filament was ultrasonically treated with alcohol and acetone for 10 min to remove dirt and pollutants on the fiber surface, and the treated PA6 fiber was then dried naturally. Second, MWCNTs were dispersed in distilled water by ultrasound for 1 h in the presence of sodium dodecyl benzene sulfonate (SDBS) as a surfactant, with a mass ratio of MWCNT/SDBS/water/alcohol = 1:1:50:50. The dried PA6 fiber was soaked in the MWCNT dispersion to obtain MWCNT/PA6-modified fiber. In a third step, the MWCNT/PA6 fiber was dried at room temperature, the complex was immersed in a mixture of pyrrole monomer and solution A consisting of sodium anthraquinone-2-sulfonate and water at 0–4 °C, and the solution was then stirred at 600 rpm for 10 min. Meanwhile, under the same volume of solution A, solution B composed of 5-sulfosalicylic acid dihydrate and iron (III) nitrate nonahydrate aqueous solution [29] was prepared. After solution B was added dropwise to solution A, the reaction solution was stirred for 4 h at 600 rpm and 0–4 °C. The fiber was removed, washed with deionized (DI) water and alcohol, and then dried naturally to obtain the PPy/MWCNT/PA6 fiber. The preparation process for the PPy/PA6 fiber was the same as for PPy/MWCNT/PA6.

Fabrication of gate electrode and Immobilization of the enzyme

To prepare the Nafion-LOx/PPy/MWCNT/PA6 and Nafion-LOx/Pt gate electrodes, PPy/MWCNT/PA6 fibers and Pt wires (1–1.5 cm) were removed and soaked in 10 mg/mL LO_X solution, prepared by phosphate-buffered saline (PBS) solutions

(pH = 6.5) for 12 h at 4 °C, followed by removal of the fiber and immersion in Nafion solution (1 wt%) for 12 h at 4 °C. Finally, the fiber and gate electrodes were removed and dried at 4 °C to obtain the LO_X-modified PPy/MWCNT/PA6 and Pt gate electrode, which were rinsed with DI water to remove residues and stored at 4 °C for future use. Lactate (1 nM–1 mM) was prepared in solution with different concentrations of PBS.

Device characterization

The electrical response of the FECTs was characterized by a Keithley 4200 semiconductor analyzer. All electrical measurements were carried out under ambient conditions. For output measurements, the channel current I_{ds} was measured as a function of drain voltage V_{ds} under gate voltage from −0.4 to 3 V. For transfer measurements, the channel current I_{ds} was measured as a function of gate voltage V_g under a constant drain voltage (V_{ds} = −2 V). Lactate detection of the FECTs in PBS solutions was carried out utilizing channel current vs. time curves (I_{ds} vs. time) at a fixed gate voltage (V_g = 1 V).

Results and discussion

Lactate sensor based on FECTs

Scheme 1a shows the fabrication of the FECTs. The nylon fiber is firstly wound in a loop, then placed in the dispersed solution of MWCNT in the presence of surfactants. The dispersion of MWCNT showed no aggregation of particles for at least 24 h after ultrasound treatment, indicating uniform stability. After treatment with MWCNT, the color of the PA6 fiber changed from white to black (Fig. 1); then polypyrrole was polymerized in situ on the surface of the MWCNT-treated fiber. The source-to-drain channel and the gate electrode were connected through the solid electrolyte consisting of mobile ions. Scheme 1b shows the preparation process of the lactate sensor, which is immobilized in the Nafion matrix with a gate electrode of either platinum or modified conductive fiber coated with lactate oxidase (LOx).

The FECT sensor is similarly assembled by adding solid electrolyte between the PPy/MWCNT/PA6 as active layer and the Pt gate electrodes. When the sensor comes into contact with the lactate solution, the gate reacts with the electrolyte, inducing a current change in the channel. Most importantly, the sensor can be woven and stitched into the fabric, which holds promise for use in wearable electronics.

Surface morphology of fibers

The surface morphology of the fibers is shown in Fig. 2. Figure 2a shows the microstructure of the original nylon fiber, which is composed of multiple monofilaments. The surface of the fiber is very smooth after cleaning, with an average diameter of 120 um. After MWCNT treatment, the cylindrical nanotubes were highly compact and evenly distributed on the fiber surface (Fig. 2b), with a diameter of 20–30 nm and a length of 10–20 um. Pure PPy without MWCNT treatment was directly polymerized on the nylon surface, showing a typical granular structure and a small number of coexisting lines (Fig. 2c). In Fig. 2d, after MWCNT treatment and in situ polymerization of pyrrole, the surface of the MWCNT/PA6 fiber forms a uniform three-dimensional linear structure. Figure 2e is a high-magnification image of (d). It shows a large area of entangled and highly dense networking structure of PPy with nanowires about 200 nm in diameter, which completely cover the surface of the MWCNT/PA6 fiber. Figure S1 (see Electronic Supplementary Material, ESM) of Infrared spectroscopy (IR) also confirms the formation of PPy. Three-dimensional interconnect PPy is wrapped around the MWCNT, which facilitates efficient carrier transfer between the fibers. Compared with the PPy/PA6 fiber system, the MWCNT becomes a soft template to absorb more pyrrole monomer, leading to the linear growth of polypyrrole between the fiber and polypyrrole, while the MWCNT also act as "bridges" connecting different filaments into a complete entity.

This is more conducive to the efficiency of carrier transport, the stability of the device, and the sensitivity of lactate determination. As displayed in Fig. 2f, the cross-sectional view clearly shows that the diameter of the fiber is about 180 um, and is composed of 15–20 nylon filaments (core) and a composite layer (shell) less than 1 um thick.

Mechanical properties and sewing of fibers

Figure 3a shows the optical images of the PPy/MWCNT/PA6 fiber under different bending conditions, indicating that the fiber is flexible and can tolerate mechanical deformation. The fiber length of the lactate sensor is 1–2 cm. As shown in Fig. 3b, the PPy/MWCNT/PA6 fiber of 2 cm was taken as an example. Under stable voltage of 2 V, the current of the fiber at bending angles from 0 to 180° remained constant. The resistance of the 2 cm fiber was calculated at about 660 Ω, and there was little change with varied time. The value agreed well with Fig. S2 (see ESM). This is attributed to the flexibility and stability of the PPy/MWCNT/PA6 fiber, resulting in no changes in the resistance under different degrees of bending. This is beneficial for future applications of the transistor devices. Figure 3c shows the results of the 2 cm PPy/MWCNT/PA6 fiber under alternating bending tests of different frequencies. Even after bending 20, 60, 100, 150, 200 times, the resistance of the conductive fiber shows only a slight increase. Moreover, the scanning electron microscopy (SEM) image in Fig. S3 (see ESM) shows no cracks appearing on the surface of the fiber after 200 cyclic bending tests. These

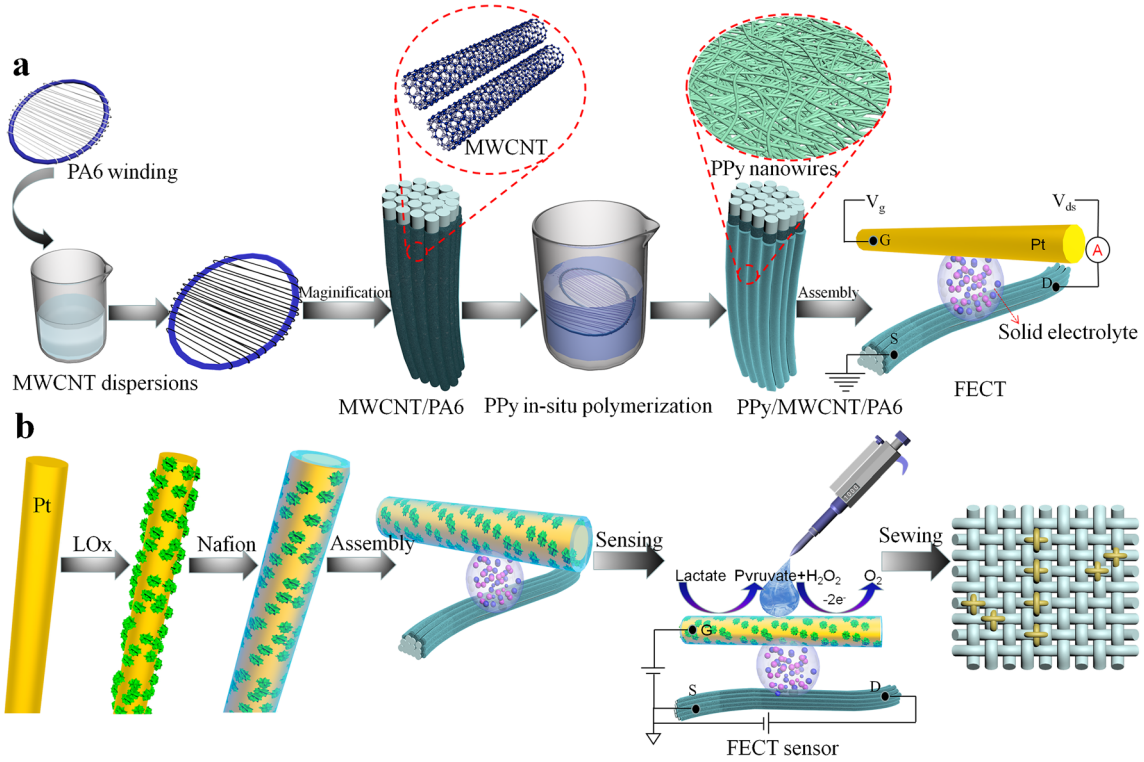

Scheme 1 Schematic illustration of the preparation process of (**a**) the fiber organic electrochemical transistors based on MWCNT and polypyrrole, and (**b**) the flexible lactate sensor assembly

results indicate that the conductivity of the functional fiber is not affected by the number of bending tests or the angles. Because of weaving and body movement, these devices experience continuous mechanical stress. Therefore, the endurance of the fiber against stress needs to be evaluated. The stress–strain curves of the PA6, PPy/PA6, MWCNT/PA6, and PPy/MWCNT/PA6 fiber are shown in Fig. 3d. The maximum fracture stress of the original PA6 fiber is about 0.28 N/tex, and the elongation at break ε is 45% ± 3%. After treatment with PPy, the largest fracture stress of the fiber decreases to 0.20 N/tex, and the elongation at break ε is 30% ± 2%. After modification by MWCNT and PPy, the maximum fracture stress is about 0.18 N/tex, and the elongation at break ε is 25% ± 1%. This indicates a decrease in Young's modulus compared to the untreated fiber. However, it can still tolerate hand-weaving, sewing, and embroidering.

Figure 3e, f shows the optical image of the PPy/MWCNT/PA6 fiber sewn into the sleeve and back of a T-shirt. The conductive fiber arrays are completely embedded in the textiles or garments. It maintains good flexibility that can withstand the human body's different angles of bending and stretching many times, demonstrating its wearability. Transistors made of the fiber can tolerate significant stress and versatile deformation. Obviously, such transistors can be integrated into wearable textiles and easily adapted to biochemical-related electrochemical sensors.

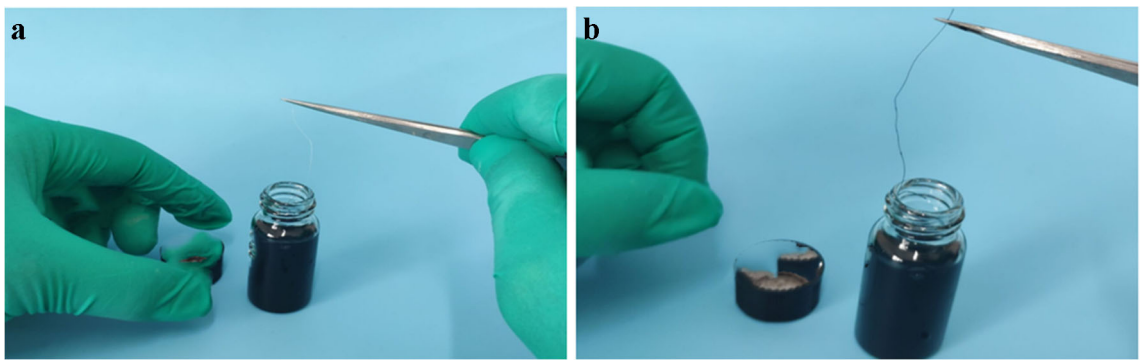

Fig. 1 The PA6 fiber before (**a**) and after (**b**) MWCNT treatment

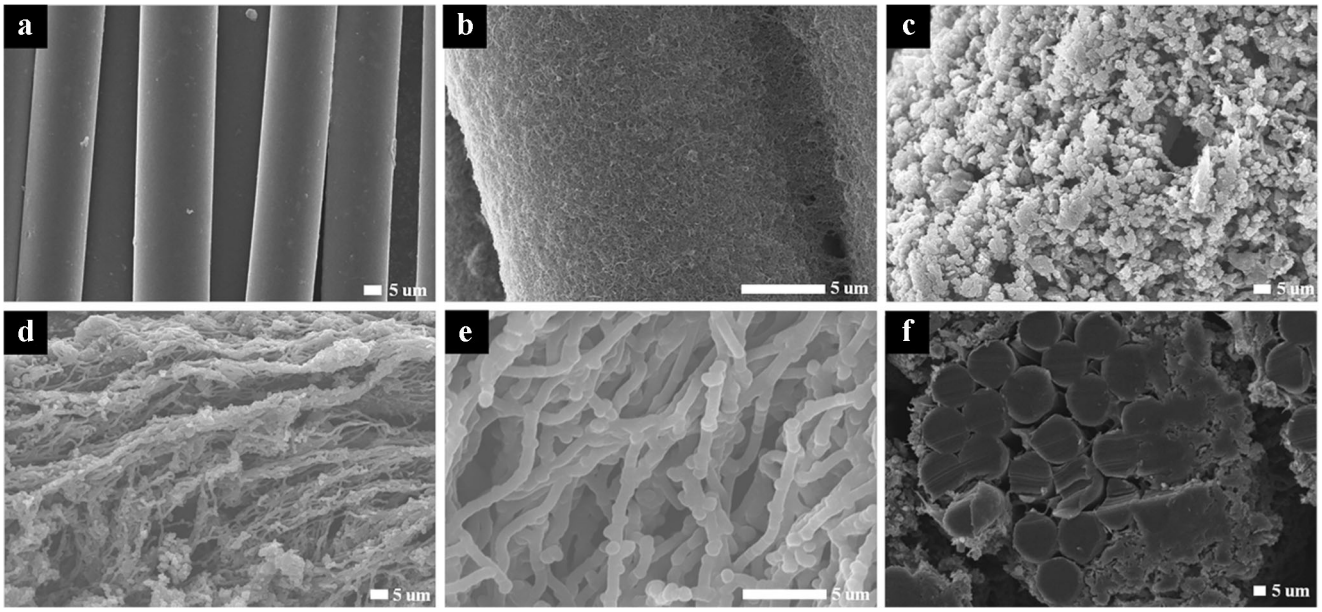

Fig. 2 SEM images of original and modified fiber. (**a**) Nylon fiber, (**b**) MWCNT/PA6 fiber, (**c**) PPy/PA6 fiber, (**d**) PPy/MWCNT/PA6 fiber, (**e**) magnification of (d, f). The cross-sectional view of the PPy/MWCNT/PA6 fiber

Electrical performance of FECTs

Figure 4a–c shows the typical output characteristics of the FECTs based on PPy/PA6, PPy/MWCNT/PA6 (PPy/MWCNT/PA6 gate electrode), and PPy/MWCNT/PA6 (Pt gate electrode), respectively. Low-voltage operation is utilized here, with negative voltage (−2 V) at the drain, and gate voltage varying from −0.4 to 3 V. With increasing gate voltage, the channel current decreases, while it increases as the source–drain voltage increases, which represents a typical depletion-mode behavior of OECTs [14, 30]. The operational mechanism of FECTs can be understood as follows: A positive voltage is applied to the gate, the cation from the electrolyte is then injected into the PPy and MWCNT channel, and finally compensates for the anions on the PPy. This leads to a decrease in the hole density in the channel, which leads to a decrease in the drain current. The output of the FECTs based on PPy/PA6, PPy/MWCNT/PA6 (PPy/MWCNT/PA6 gate electrode), and PPy/MWCNT/PA6 (Pt gate electrode) was investigated separately. Compared with PPy/PA6, the MWCNT modification significantly increased the on-current of the devices from 14 mA to 25 mA. Figure 4d–f displays the transfer curves of PPy/PA6, PPy/MWCNT/PA6 (fiber gate electrode), and PPy/MWCNT/PA6 (Pt gate electrode). Compared with other devices, the FECTs based on composites with a Pt modified gate electrode exhibit the highest slope of the transfer curve. The transfer curve of the FECTs with MWCNT and PPy composites shows that the channel current changes by two orders of magnitude under gate voltages from 0 to 3 V. The on/off ratios of the three devices are calculated as 30, 67, 102, respectively. The FECTs based on the PPy/PA6 fiber show an on/off current ratio of 30. However, the FECTs based on the PPy/MWCNT/PA6 fiber exhibit higher on-current and lower off-current, leading to a higher on/off ratio. Figure 4g–i demonstrates that all FECTs can be turned on and off rapidly on a 0.5-s time scale. The devices are in the on-state at $V_g = 0$ V and in the off-state at $V_g = 2.7$ V. After switching between on–off states many times, the cycle stability of the PPy/PA6 devices is decreased. By contrast, the Pt gate electrode based on the PPy/MWCNT/PA6 device exhibits the most outstanding performance, indicating good signal modulation between on- and off-states. This may be attributed to the electrochemical activity of Pt, which has a larger active surface area than the other electrodes.

Working principle of FECT-based lactate sensors

When the applied gate voltage reaches 1.0 V and the solution of different lactate concentrations is dropped onto the gate electrode, lactate is oxidized to pyruvate and lactate oxidase is reduced, as shown in Eq. (1) [31, 32]. The oxidation process results in the donation of electrons to the gate electrode, generating a Faraday current and changing the double electrical layer at the gate/electrolyte interface, which decreases the voltage drop at the gate/electrolyte and increases the gate voltage at the electrolyte/channel, hence inducing an increase in the effective gate voltage and directly affecting the channel current I_{ds} [33, 34]. The schematic illustration of the potential drop before and after the addition of lactate is shown in Fig. 5.

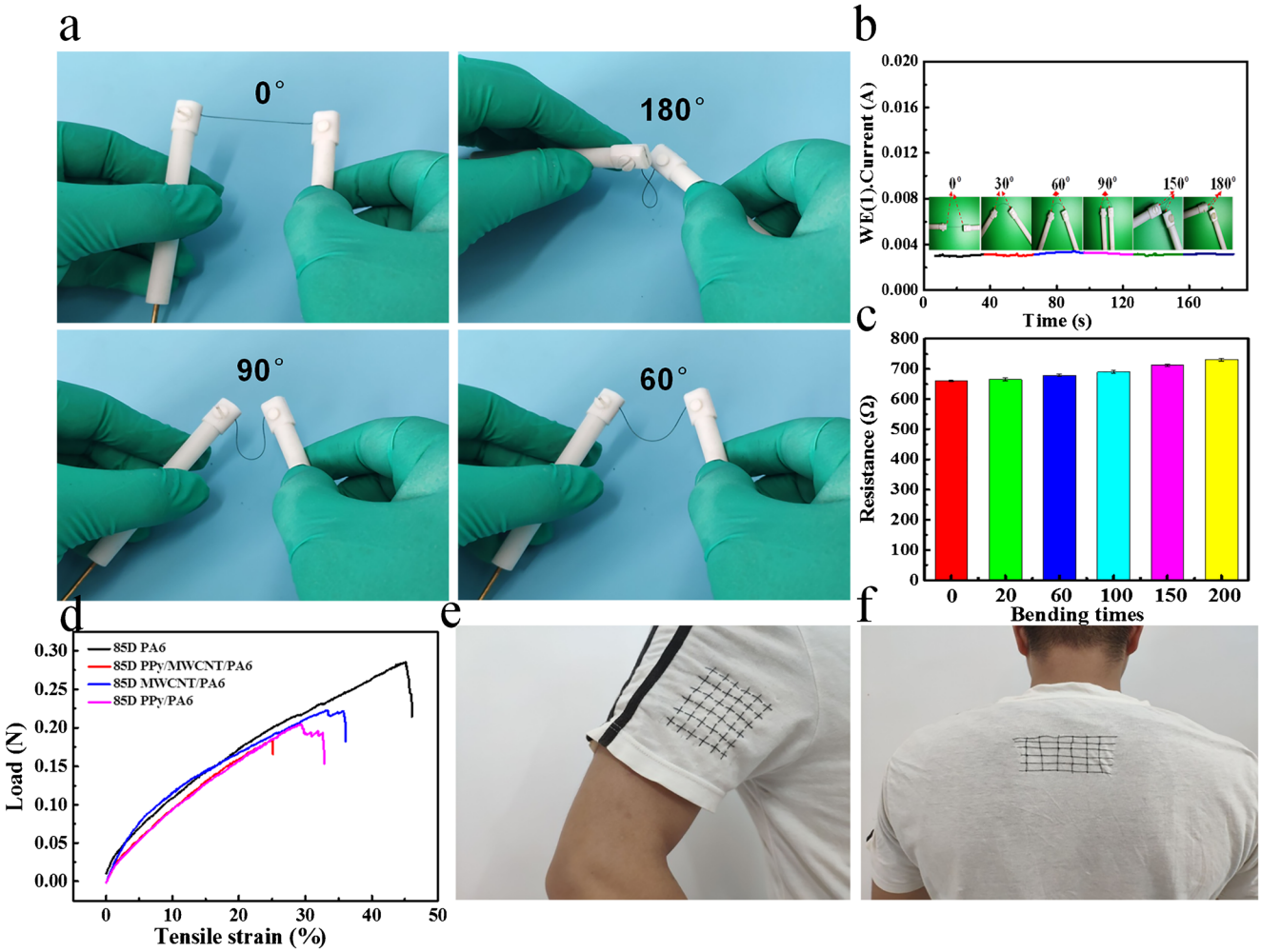

Fig. 3 (**a**) Digital photographs of the fiber from extending to bending states, (**b**) current vs. time relationship and the image of bending to different angles, (**c**) resistance as a function of bending time, (**d**) load and stress curves of different fibers. Optical image showing the PPy/MWCNT/PA6 fiber array sewn into the (**e**) sleeve and (**f**) back of a T-shirt

$$L\text{–}Lactate + O_2 \overset{LO_X}{\rightarrow} Pyruvate + H_2O_2 H_2O_2 \rightarrow 2H^+ + O_2 + 2e^- \quad (1)$$

In fiber organic electrochemical transistor devices, the Faraday-induced current increases the effective gate voltage of the transistor. In general, the calculation formula for the channel current of organic electrochemical transistors is expressed by Eq. 2 [18, 33, 35] as follows.

$$I_{ds} = \frac{Wq\mu tp_o}{LV_p}\left(V_p - V_g^{eff} + \frac{V_{ds}}{2}\right)V_{ds}, \left(|V_{ds}| << \left|V_p - V_g^{eff}\right|\right)V_p \quad (2)$$
$$= \frac{qtp_0}{C_i}V_g^{eff} = V_g + V_{offset}$$

where W and L represent the width and length of the channel, t is the thickness of the organic semiconductor layer (PPy and MWCNT), q is the electronic charge (1.602×10^{-19}), μ is the hole mobility, C_i is the effective gate capacitance, p_o is the initial hole density of the channel before V_g is applied, V_p is the clipping voltage, and V_{ds} is the source–drain voltage. V_g^{eff} represents the effective gate voltage in the device, and V_{offset} is the potential change caused by the potential difference between the Pt/electrolyte and the PPy and MWCNT composite/electrolyte interface.

In this study, PBS solution (pH = 6.5) is utilized to dilute lactate to prepare lactate solution at concentrations of 1 nM/L, 50 nM/L, 100 nM/L and 1 uM/L, 100 uM/L, 1 mM/L. Then the fixed lactate enzyme electrode is added to test the sensitivity of the lactate sensor. From the following Eq. (3), it can be concluded that when V_g^{eff} increases with the increase in lactate (LA) concentration, I_{ds} is gradually reduced [15, 36].

$$V_g^{eff} = \frac{2.3(1+r)kT}{ne}\log[C_{LA}] + \text{constant} \quad (3)$$

where r is the ratio between the capacitance of the electrolyte/

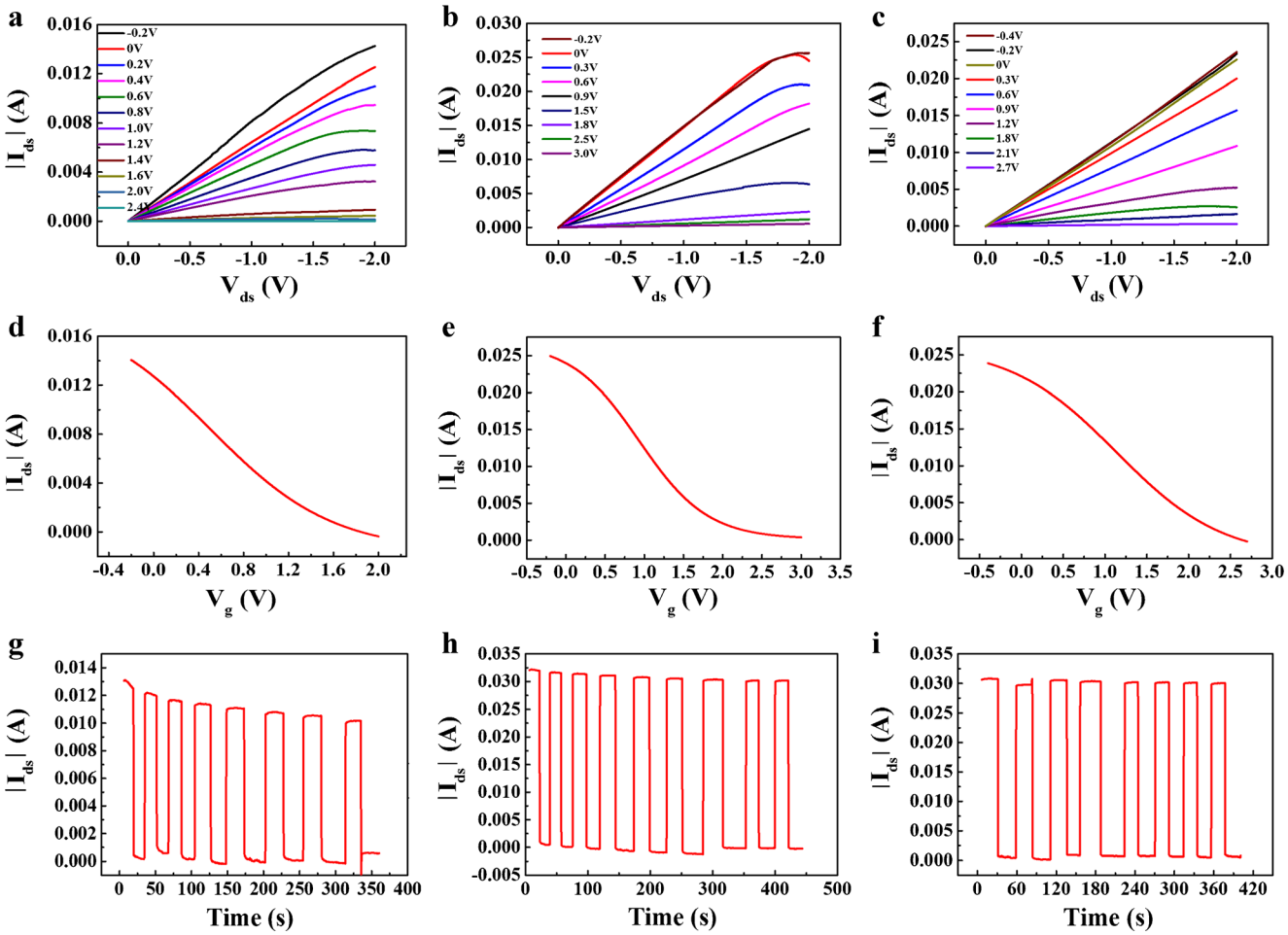

Fig. 4 Output characteristics of FECTs based on (**a**) PPy/PA6 with PPy/PA6 gate electrode, (**b**) PPy/MWCNT/PA6 with PPy/MWCNT/PA6 gate electrode, and (**c**) PPy/MWCNT/PA6 with Pt gate electrode. Transfer characteristics of FECTs based on (**d**) PPy/PA6 with PPy/PA6 gate electrode, (**e**) PPy/MWCNT/PA6 with PPy/MWCNT/PA6 gate electrode, and (**f**) PPy/MWCNT/PA6 with Pt gate electrode. Transient characteristics of FECTs based on (**g**) PPy/PA6 with PPy/PA6 gate electrode, (**h**) PPy/MWCNT/PA6 with PPy/MWCNT/PA6 gate electrode, and (**i**) PPy/MWCNT/PA6 with Pt gate electrode

channel (C_c) and the electrolyte/gate interface (C_g), $r = C_c/C_g$, k is the Boltzmann constant, T is the temperature, and C_{LA} is the concentration of lactate. By detecting the changes in channel current or effective gate voltage, the lactate concentration in the analyte can be obtained.

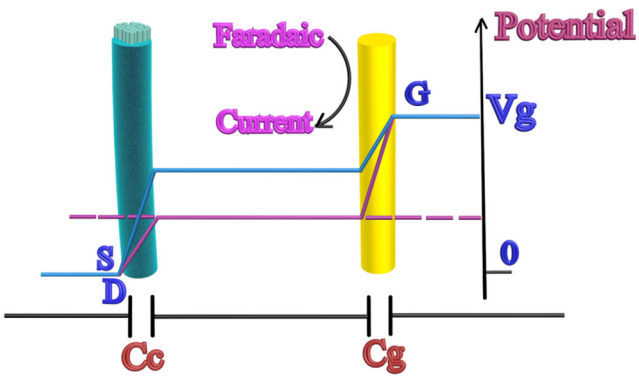

Fig. 5 The potential drop between the Pt gate and PPy/MWCNT channel before (red line) and after (blue line) the addition of lactate in PBS solution

Sensing performance of lactate

Figure 6a and b demonstrate the real-time current responses of the FECTs with Nafion-LOx/PPy/MWCNT/PA6 and Nafion-LOx/Pt gate electrode to the addition of lactate continuously with varying concentrations. Through the different current responses under the varied concentrations of lactate, the lactate sensor is sensitive to the performance when the external gate voltage set for this test is 1.0 V. To determine the better gate material, the FECT performance with different Pt gate electrodes and PPy/MWCNT/PA6 was evaluated. Both devices presented a current response to 1 nM lactate, and the response time was 0.6–0.8 s, while the response was significantly enhanced with increased lactate concentration. In the case of the conductive fiber gate electrode, the current response was more obvious after adding the 1 nM lactate than that of the Pt gate electrode. When lactate concentration was increased, the channel current I_{ds} continued to

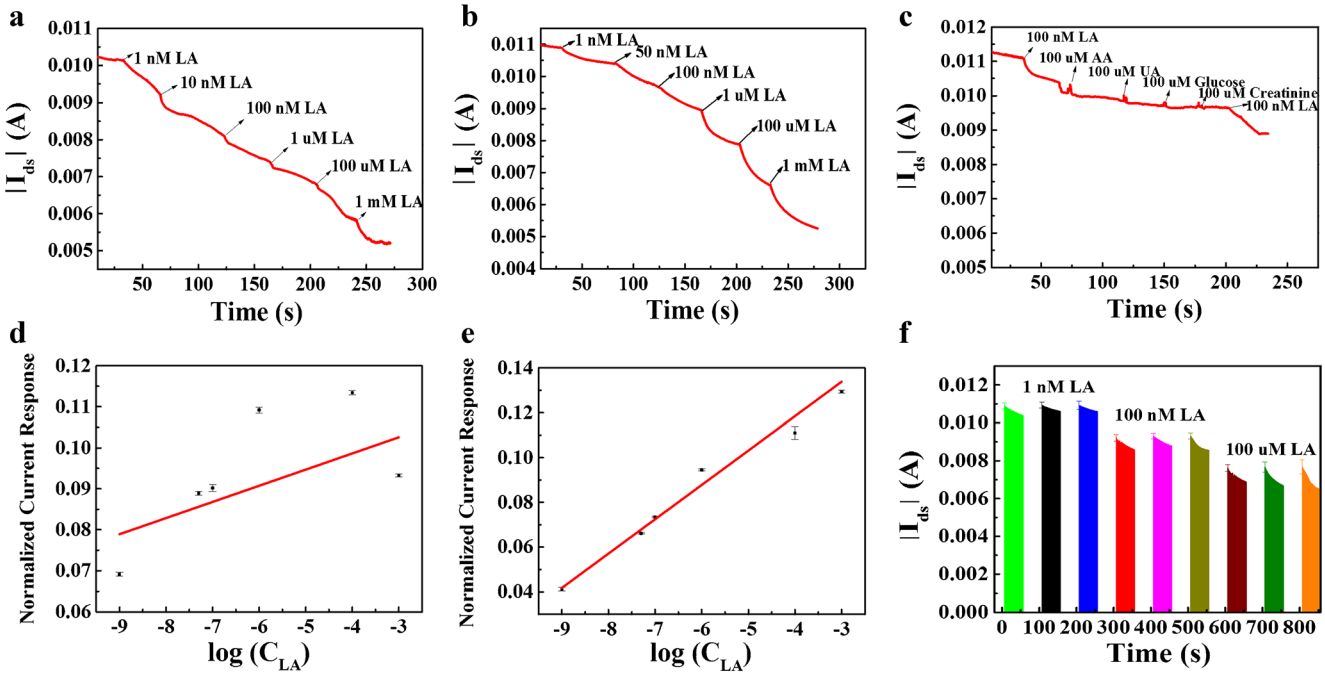

Fig. 6 Sensing performance of the FECTs with (**a**) Nafion/PPy/MWCNT/PA6 and (**b**) Nafion/Pt gate electrode for lactate (LA) concentrations from 1 nM to 1 mM at $V_{ds} = -1$ V, with V_g is fixed at 1 V. (**c**) Selectivity measurements of the FECTs with the Pt gate using the addition of 100 nm lactate intercalated by the addition of 100 uM AA, 100 uM UA, 100 uM glucose, and 100 uM creatinine. The normalized current response with (**d**) Nafion/Pt and (**e**) Nafion/PPy/MWCNT/PA6 gate electrode as a function of the logarithm of lactate concentration. (**f**) The reproducibility of the FECTs with Pt gate electrode

increase. However, compared with the Pt gate electrode, the current response of the sensor based on the fiber gate electrode decreased slightly with the increase in lactate concentration. The current variation was less than 1 mA even at a high lactate concentration of 1 uM, demonstrating that the modulation signal of the sensor is weaker than that of the Pt gate sensor. The Pt gate electrode fixed with lactate oxidase provides better sensitivity for the device. The presence of Pt promotes the generation of chemical reactions and reduces H_2O_2 concentration, resulting in the possibility of donating more electrons near the surface of the gate electrode. In addition, the linear regime for the desired sensitivity range is of considerable importance. Linearity determines the accuracy of sensor signals, which can be evaluated by the correlation coefficient (R). To compare the response of the channel current after the addition of the lactate, the normalized current response (NCR) was calculated in accordance with Eq. 4 [37, 38]. Figure 6d and e show the NCR curves of the FECT-based lactate sensors in response to different concentrations of lactate solution.

$$NCR = \left| \frac{I_D^{conc} - I_D^{conc=0}}{I_D^{conc=0}} \right| \tag{4}$$

where $I_D^{conc=0}$ and I_D^{conc} are the channel currents before and after the addition of lactate solution, respectively. As seen in Fig. 6d, when the concentration of lactate increases from 1 nM to 10 uM, compared with the PPy/MWCNT/PA6 electrode (correlation coefficient at 0.5856), the calibration curve (linear regime) for the Pt gate electrode has better curve fitting, with a correlation coefficient of 0.9889. Sensitivity of 0.15 NCR per decade is obtained for the Pt gate-based sensors, which is almost three times that of the PPy/MWCNT/PA6 gate electrode, further illustrating the greater sensitivity and stability of Pt for the gate device.

The improvement in the device sensitivity can be attributed to the larger active surface area and higher electrocatalytic activity of the Pt gate electrode [15]. Compared with the fiber electrode, it can improve the efficiency of charge transfer on the gate electrode, promote fast electrochemical reaction, and determine the sensing ability of devices. The results indicate that the Pt gate yields better sensitivity in the sensing range, so the Pt gate-based devices are used in the subsequent performance test.

The selectivity of the FECT sensor is of considerable importance for biosensors. The biological fluid including the lactate coexists with interfering species such as uric acid (UA), amino acid (AA), glucose, and creatinine. Analysis was performed to assess whether these substances would interfere with the determination of lactate. Figure 6c shows the specificity of the FECTs with a Nafion-LOx/Pt gate electrode. The 100 uM uric acid (UA), 100 uM amino acid (AA), 100 uM creatinine, 100 uM glucose solution, and 100 nM lactate were selected and compared. When 100 nM lactate was added, the channel current response decreased rapidly to a certain extent. However, when

a high concentration of AA, UA, glucose, and creatinine was injected into the devices, almost negligible current response was observed, as shown in Fig. 6c. Subsequently, after additional 100 nM lactate was added, I_{ds} showed a significant change and kept the same amplitude as before. These results indicate that the FECT sensor with a Nafion-LOx/Pt gate electrode remains free of potentially interfering species and has good selectivity to lactate, thus providing a promising platform for selective detection of lactate in real samples. Reproducibility is considered a crucial factor for biosensor performance. To investigate the reproducibility of the FECT sensors, nine devices were fabricated separately under similar procedures and then evaluated by means of parallel measurements of lactate at different concentrations. The accuracy of the sensitive performance of the lactate sensor was analyzed through the test results. As shown in Fig. 6f, all the measured values of the three groups of lactate sensors tested have high matching with their respective current responses. At different concentrations, the calculated relative standard deviation of these repetitive measurements is in the range of 1.68–3.93%, indicating that the sensors based on FECTs have satisfactory reproducibility.

Analysis of real samples

The development of a noninvasive method for the determination of lactate is of great significance. People who engage in strenuous physical activity for a short period are reported to have about 537 nM of lactate in their sweat [39]. To demonstrate the practicality of the prepared FECT sensor, the direct analysis of lactate concentration in human sweat after exercise was investigated by applying the standard addition method. Sweat samples were collected from four healthy volunteers after physical exercise, then diluted with PBS solution and mixed with the 537 nM concentration of standard liquid. Finally, the mixture solution was added to the lactate sensor. Table 1 and ESM Fig. S4 show the results for these prepared sensors. The calculated relative standard deviation after recovery is 5.57%, and the recovery values of lactate range from 96.8% to 109.3%. These results indicate that our lactate sensor can detect the content of lactate in body fluids to evaluate the level of exercise intensity, which can be applied in future biological and healthcare detection.

Table 1 Determination results of the real samples and recovery

Sample content (10^{-7} mol/L)	Added (10^{-7} mol/L)	Measured (10^{-7} mol/L)	Recovery (10^{-7} mol/L)	RSD (%)
5.37	5.37	11.10	100.2	5.57
		10.57	96.8	
		10.88	102.6	
		11.24	109.3	

Note: RSD represents relative standard deviation

Conclusions

In summary, fiber organic electrochemical transistors based on polypyrrole and multi-walled carbon nanotube composites were prepared and used as biosensors to detect lactate. The MWCNT provided a larger surface area for functionalization, while the synergistic effect of MWCNT and PPy nanowires enhanced the electrical properties and sensing performance. To further enhance the sensing properties, different gate electrode modifications were investigated. The proposed biosensor demonstrated advantages of fast response, high sensitivity, and good specificity, as well as outstanding stability and repeatability. Based on the superior sensitivity of the proposed device, the noninvasive testing of human sweat after exercise was successfully carried out. We believe that the fiber organic electrochemical transistor-based sensor with appropriate functionalization can be applied as an ideal platform for ultrasensitive and portable detection of analytes in real samples for healthcare and biological applications. In addition, the sensors can be woven and stitched into fabrics, and can thus play an important role in the development of wearable devices for biomedical applications.

Acknowledgments This work was supported by the National Natural Science Foundation of China (grant nos. 51503157, 51873166, and 51603155), the Program for Provincial and Ministerial Base Platform of Hubei (2017AHB065), and the Science & Technology Program of Wuhan Technology Bureau (2017060201010165). The authors acknowledge financial support from the Hubei Province Education Department Project (Q20191708), Wuhan Advanced Fiber Engineering Technology Research Center and the Hubei Province Central Government Guides Local Science and Technology Development Projects (2018ZYYD057). The authors also acknowledge Jia Xu for revision and correction work on this paper.

Compliance with ethical standards

All the experiments were carried out with the approval of the laboratory ethics committee of Wuhan Textile University. Informed consent was obtained from all individual participants included in the study.

Conflict of interest The authors declare that they have no conflict of interest.

References

1. Bakker J, Gris P, Coffernils M, Kahn RJ, Vincent JL. Serial blood lactate levels can predict the development of multiple organ failure following septic shock. Am J Surg. 1996;171:221–6.
2. Ackland MR, Reeder JE. A rapid chemical spot test for the detection of lactic acid as an indicator of microbial spoilage in preserved foods. J Appl Bacteriol. 1984;56:415–9.
3. Lee DK, Jang S, Baek EH, Kim MJ, Lee KS, Shin HS, et al. Lactic acid bacteria affect serum cholesterol levels, harmful fecal enzyme activity, and fecal water content. Lipids Health Dis. 2009;8:21.
4. Perdigón G, Maldonado Galdeano C, Valdez JC, Medici M. Interaction of lactic acid bacteria with the gut immune system. Eur J Clin Nutr. 2002;56:S21–S6.

5. Soldà A, Valenti G, Marcaccio M, Giorgio M, Pelicci PG, Paolucci F, et al. Glucose and lactate miniaturized biosensors for SECM-based high-spatial resolution analysis: a comparative study. ACS Sensors. 2017;2:1310–8.
6. Bariskaner H, Ustun ME, Ak A, Yosunkaya A, Dogan N, Gurbilek M. Effects of deferoxamine on tissue lactate and malondialdehyde levels in cerebral ischemia. Methods and findings in experimental and clinical pharmacology. Methods Find Exp Clin Pharmacol. 2003;25:371–6.
7. Posner BA, Li L, Bethell R, Tsuji T, Benkovic SJ. Engineering specificity for folate into dihydrofolate reductase from escherichia coli. Biochemistry. 1996;35:1653–63.
8. Suh SW, Aoyama K, Chen Y, Garnier P, Matsumori Y, Gum E, et al. Hypoglycemic neuronal death and cognitive impairment are prevented by poly(ADP-ribose) polymerase inhibitors administered after hypoglycemia. J Neurosci. 2003;23:10681.
9. Martí R, Varela E, Segura RM, Alegre J, Suriñach JM, Pascual C. Determination of D-lactate by enzymatic methods in biological fluids: study of interferences. Clin Chem. 1997;43:1010.
10. Ross JM, Öberg J, Brené S, Coppotelli G, Terzioglu M, Pernold K, et al. High brain lactate is a hallmark of aging and caused by a shift in the lactate dehydrogenase a/B ratio. Proc Natl Acad Sci U S A. 2010;107:20087.
11. Sun H, Gerasimov J, Berggren M, Fabiano S. N-type organic electrochemical transistors: materials and challenges. J Mater Chem C. 2018;6:11778–84.
12. Duong DT, Tuchman Y, Chakthranont P, Cavassin P, Colucci R, Jaramillo TF, et al. A universal platform for fabricating organic electrochemical devices. Adv Electron Mater. 2018;4:1800090.
13. Liao C, Zhang M, Niu L, Zheng Z, Yan F. Organic electrochemical transistors with graphene-modified gate electrodes for highly sensitive and selective dopamine sensors. J Mater Chem B. 2014;2:191–200.
14. Khodagholy D, Rivnay J, Sessolo M, Gurfinkel M, Leleux P, Jimison LH, et al. High transconductance organic electrochemical transistors. Nat Commun. 2013;4:2133.
15. Ji X, Lau HY, Ren X, Peng B, Zhai P, Feng SP, et al. Highly sensitive metabolite biosensor based on organic electrochemical transistor integrated with microfluidic channel and poly(n-vinyl-2-pyrrolidone)-capped platinum nanoparticles. Adv Mater Technol. 2016;1:1600042.
16. Strakosas X, Huerta M, Donahue MJ, Hama A, Pappa AM, Ferro M, et al. Catalytically enhanced organic transistors for in vitro toxicology monitoring through hydrogel entrapment of enzymes. J Appl Polym Sci. 2017;134:44483.
17. Wang Y, Qing X, Zhou Q, Zhang Y, Liu Q, Liu K, et al. The woven fiber organic electrochemical transistors based on polypyrrole nanowires/reduced graphene oxide composites for glucose sensing. Biosens Bioelectron. 2017;95:138–45.
18. Qing X, Wang Y, Zhang Y, Ding X, Zhong W, Wang D, et al. Wearable fiber-based organic electrochemical transistors as a platform for highly sensitive dopamine monitoring. ACS Appl Mater Interfaces. 2019;11:13105–13.
19. Qian T, Yu C, Wu S, Shen J. A facilely prepared polypyrrole–reduced graphene oxide composite with a crumpled surface for high performance supercapacitor electrodes. J Mater Chem A. 2013;1:6539–42.
20. Biswas S, Drzal LT. Multilayered nanoarchitecture of graphene nanosheets and polypyrrole nanowires for high performance supercapacitor electrodes. Chem Mater. 2010;22:5667–71.
21. Zhang J, Yu Y, Liu L, Wu Y. Graphene–hollow PPy sphere 3D-nanoarchitecture with enhanced electrochemical performance. Nanoscale. 2013;5:3052–7.
22. Pan X, Chen X, Li Y, Yu Z. Facile synthesis of Co_3O_4 nanosheets electrode with ultrahigh specific capacitance for electrochemical supercapacitors. Electrochim Acta. 2015;182:1101–6.
23. Lu X, Yu M, Wang G, Tong Y, Li Y. Flexible solid-state supercapacitors: design, fabrication and applications. Ener Environ Sci. 2014;7:2160–81.
24. Sheng Q, Wang M, Zheng J. A novel hydrogen peroxide biosensor based on enzymatically induced deposition of polyaniline on the functionalized graphene–carbon nanotube hybrid materials. Sensor Actuat B-Chem. 2011;160:1070–7.
25. Yun Y, Dong Z, Shanov VN, Schulz MJ. Electrochemical impedance measurement of prostate cancer cells using carbon nanotube array electrodes in a microfluidic channel. Nanotech. 2007;18:465505.
26. Cui X, Li CM, Zang J, Zhou Q, Gan Y, Bao H, et al. Biocatalytic generation of PPy-enzyme-CNT nanocomposite: from network assembly to film growth. J Phys Chem C. 2007;111:2025–31.
27. Braik M, Barsan MM, Dridi C, Ben Ali M, Brett CMA. Highly sensitive amperometric enzyme biosensor for detection of superoxide based on conducting polymer/CNT modified electrodes and superoxide dismutase. Sensor Actuat B-Chem. 2016;236:574–82.
28. Xue L, Wang W, Guo Y, Liu G, Wan P. Flexible polyaniline/carbon nanotube nanocomposite film-based electronic gas sensors. Sensor Actuat B-Chem. 2017;244:47–53.
29. Wang Y, Zhou Z, Qing X, Zhong W, Liu Q, Wang W, et al. Ion sensors based on novel fiber organic electrochemical transistors for lead ion detection. Anal Bioanal Chem. 2016;408:5779–87.
30. Bernards DA, Malliaras GG. Steady-state and transient behavior of organic electrochemical transistors. Adv Funct Mater. 2007;17:3538–44.
31. Bi Y, Ye L, Mao Y, Wang L, Qu H, Liu J, et al. Porous carbon supported nanoceria derived from one step in situ pyrolysis of Jerusalem artichoke stalk for functionalization of solution-gated graphene transistors for real-time detection of lactic acid from cancer cell metabolism. Biosens Bioelectron. 2019;140:111271.
32. Samadi Pakchin P, Ghanbari H, Saber R, Omidi Y. Electrochemical immunosensor based on chitosan-gold nanoparticle/carbon nanotube as a platform and lactate oxidase as a label for detection of CA125 oncomarker. Biosens Bioelectron. 2018;122:68–74.
33. Bernards DA, Macaya DJ, Nikolou M, DeFranco JA, Takamatsu S, Malliaras GG. Enzymatic sensing with organic electrochemical transistors. J Mater Chem. 2008;18:116–20.
34. Liao C, Mak C, Zhang M, Chan HLW, Yan F. Flexible organic electrochemical transistors for highly selective enzyme biosensors and used for saliva testing. Adv Mater. 2015;27:676–81.
35. Zhang M, Liao C, Yao Y, Liu Z, Gong F, Yan F. High-performance dopamine sensors based on whole-graphene solution-gated transistors. Adv Funct Mater. 2014;24:978–85.
36. Cicoira F, Sessolo M, Yaghmazadeh O, DeFranco JA, Yang SY, Malliaras GG. Influence of device geometry on sensor characteristics of planar organic electrochemical transistors. Adv Mater. 2010;22:1012–6.
37. Tang H, Lin P, Chan HLW, Yan F. Highly sensitive dopamine biosensors based on organic electrochemical transistors. Biosens Bioelectron. 2011;26:4559–63.
38. Liao J, Lin S, Yang Y, Liu K, Du W. Highly selective and sensitive glucose sensors based on organic electrochemical transistors using TiO_2 nanotube arrays-based gate electrodes. Sensor Actuat B-Chem. 2015;208:457–63.
39. Cai X, Yan J, Chu H, Wu M, Tu Y. An exercise degree monitoring biosensor based on electrochemiluminescent detection of lactate in sweat. Sensor Actuat B-Chem. 2010;143:655–9.